applied sciences

MDPI

Article

CFD Assessment of Car Park Ventilation System in Case of Fire Event

Ramin Rahif * and Shady Attia

Sustainable Building Design Lab, Department UEE, Faculty of Applied Sciences, University of Liège, 4000 Liège, Belgium

* Correspondence: ramin.rahif@uliege.be

Abstract: This scientific article presents the results of computational fluid dynamics (CFD) simulations conducted using OpenFOAM to evaluate the effectiveness of a jet fan ventilation system in managing the dispersion of smoke resulting from a car fire incident within an underground car park spanning a total area of 21,670 m^2, situated in Tabriz, Iran. The primary objective of the study is to determine the velocity fields and evaluate visibility conditions within a 10 m radius to gauge the efficiency and effectiveness of the system. The study employs a smoke concentration production rate of 5.49×10^{-4} kg/m^3s for simulations involving fire scenarios. A total of 17 fire scenarios are examined, each extending 30 m in all directions from the initial location. The research findings demonstrate that the placement of jet fan components plays a significant role in the system's efficiency, with fans positioned near the ceiling leading to back-layering. To mitigate this issue, the recommended design solution involves the strategic installation of multiple jet fan arrays in specific zones with the addition of 10 extra jet fans, effectively curbing lateral smoke dispersion. Furthermore, the analysis of air flow rates shows that when jet fans direct an excessive airflow towards the exhaust shafts (which have a designated flow rate of 22.5 m^3/s), recirculating flows occur, leading to the dispersion of smoke throughout the car park. Consequently, the utilization of low-velocity jet fans (11.2 m/s) proves to be more effective in clearing smoke compared to high-velocity jet fans (22.3 m/s). The study also emphasizes the importance of optimal positioning of supply and exhaust shafts to achieve effective smoke control, highlighting the need for placing them on opposite walls or minimizing airflow turns. Additionally, the research underscores the significance of fire resistance in jet fan units, as their failure during fire incidents can have severe consequences.

Keywords: induction fan; jet fan; indoor air quality; fire safety; computational fluid dynamics; smoke management; impulse ventilation

Citation: Rahif, R.; Attia, S. CFD Assessment of Car Park Ventilation System in Case of Fire Event. *Appl. Sci.* **2023**, *13*, 10190. https://doi.org/10.3390/app131810190

Academic Editors: Junhong Park and Jing Zhao

Received: 11 July 2023
Revised: 22 August 2023
Accepted: 4 September 2023
Published: 11 September 2023

1. Introduction

The exponential growth of the automobile population presents a pressing issue for car parking spaces, particularly in commercial buildings. To meet this demand, large multi-storey and underground car parks have emerged as viable solutions [1]. However, it is crucial to recognize the significance of indoor air quality (IAQ) within underground car parks, as it directly impacts human health. Prolonged exposure to poor IAQ in these environments can have adverse effects on individuals [1]. Additionally, the restricted height characteristic of underground car parks poses challenges during fire incidents, as the rapid descent of the smoke layer hinders evacuation, search, and rescue operations [2]. This highlights the importance of effective ventilation systems in underground car parks to mitigate health risks associated with inhaling combustion byproducts, such as carbon monoxide (CO), which commonly serves as an indicator of indoor air quality in these facilities [3]. Furthermore, ensuring people's safety during unforeseen fire events becomes a critical consideration.

Traditional ventilation methods in underground car parks have historically relied on a ductwork system to exhaust contaminated air and introduce fresh air [3]. However,

this approach is associated with high costs, necessitates extensive equipment, occupies significant space, and results in substantial head losses [3]. Recently, a novel mechanical ventilation system has emerged, utilizing jet fans (also termed as impulse fans or induction fans) mounted beneath the car park ceiling, known as positive pressure ventilation (PPV). This approach draws inspiration from the use of jet fans for longitudinal ventilation in tunnels [4]. While one-dimensional flow is commonly assumed in tunnel applications, the ventilation dynamics in underground car parks, where flow conditions are approximately isothermal, predominantly occur in two dimensions. Consequently, the design of such ventilation systems becomes more intricate [3].

The integration of jet fan ventilation systems into car park and tunnel ventilation holds substantial promise for advancing the concept of carbon neutrality. These systems have been shown through empirical evidence to exhibit a heightened level of energy efficiency when compared to traditional methods [5,6]. This observation gains even greater significance within the current landscape, characterized by a discernible shift towards the replacement of conventional systems with environmentally conscious alternatives. This collective effort seeks to amplify the pursuit of carbon neutrality, particularly within the realm of building design and infrastructure development [7–12]. In the context of this trend, the adoption of jet fan ventilation systems serves as a notable example of embracing innovative solutions to achieve heightened sustainability goals and mitigate global warming.

The design complexity of jet fan ventilation systems necessitates the use of computational fluid dynamics (CFD) to model airflow within the car park and ensure optimal design effectiveness. CFD simulations provide a sophisticated and comprehensive tool for analyzing systems involving heat and mass transfer through computer models [13], offering insights into flow fields that would otherwise be challenging to visualize [14]. The numerical approach of CFD enables the prediction of fluid flow characteristics, including velocity, temperature, and pressure. Moreover, it allows for the extension of these predictions to forecast other factors, such as visibility, which can be compromised by smoke generated during a fire incident. In recent years, CFD modeling has become indispensable for studying large-scale underground car parks, facilitating assessments of air quality and the prediction of smoke and heat propagation in the event of a fire.

Some studies have been conducted to analyze the performance of jet fan ventilation systems using numerical approaches. Çakir and Ün [15] examined the effectiveness of jet fan ventilation systems in controlling smoke and temperature in an underground car park located in Isparta, Turkey. Utilizing Ansys 18.2 software, their analysis revealed that the smoke dissipated in under five minutes from the majority of areas, with temperatures consistently below 60 °C, ensuring visibility of over five meters throughout the car park. Sittisak et al. [16] investigated the effectiveness of single and twin jet fan installations in removing CO gas in Bangkok, Thailand. They discovered that jet fans were successful in reducing harmful CO gas levels, with the most optimal setups consisting of 43 straight twin jet fans with a 1.5 m gap distance and 23 inclined single jet fans. The efficiency of CO removal was affected by energy loss in the air stream and the gap distance between the fans. Taking into account both ventilation efficiency and energy utilization, the inclined single jet fan emerged as a promising choice. Sultansu and Onat [17] numerically analyzed ventilation and smoke control of jet fan system in a garage with a capacity of 38 cars. Through CFD analyses, it was determined that the concentration of CO and air velocity profiles were influenced by the car occupancy rate and the hanging heights of the jet fans. Optimization of the jet fan hanging heights was found to be crucial in achieving effective CO exhaust and ventilation. In the context of the SARS-CoV-2 epidemic, Nazari et al. [18] conducted a study using the OpenFOAM C++ libraries to examine the influence of jet fans on the spread of the virus in an underground car park in Tabriz, Iran. To mitigate viral transmission, the authors recommend the establishment of safe pathways near fresh air ducts, considering the flow patterns generated by the jet fans. Additionally, the study suggests equipping jet fans with ultraviolet light emitters and high-efficiency

particulate air (HEPA) filters as effective strategies for eliminating viruses. In addition to the abovementioned studies, some similar studies exist [19–23] that are summarized in Table 1.

Table 1. Summary of numerical studies on evaluation of jet fan ventilation system performance.

Author(s) and Year of Publication	Ref.	Location	Building Type	Focus: Normal Conditions (N)/Fire Events (F)
Nazari et al., 2021	[18]	Tabriz, Iran	Commercial	N
Çakir and Ün, 2020	[15]	Isparta, Turkey	Hospital	F
Sittisak et al., 2020	[16]	Bangkok, Thailand	Commercial and office	N
Sultansu and Onat, 2020	[17]	Turkey	n/d	N and F
Kmecová et al., 2019	[19]	Slovakia	Commercial	F
Špiljar et al., 2018	[22]	Croatia	n/d	N
Immonen, 2016	[20]	Finland	n/d	N
Senveli et al., 2015	[21]	Istanbul, Turkey	Business center	N and F
Deckers et al., 2013	[23]	Ghent, Belgium	Industrial	F

Despite existing numerical studies on jet fan ventilation systems in car parks, there is a need for additional research to enhance and supplement previous findings. Previous studies often focused on small-scale car parks or considered a limited number of fire scenarios to minimize computational costs. Additionally, limited attention has been given to analyzing visibility conditions following smoke propagation in car parks after fire incidents. To address these knowledge gaps, this paper aims to provide practical insights into jet fan ventilation design, with a focus on safeguarding human health during unforeseen fire events in underground car parks. The research questions to be addressed are as follows:

- What is the impact of adding an appropriate number of jet fan lines on the ventilation system's capability to prevent back-layering and lateral smoke dispersion?
- How does the comparison of jet fan airflow rates between the high and low velocity jet fans affect the dispersion of smoke in underground car parks?
- What is the impact of the optimal positioning of supply and exhaust shafts on achieving efficient ventilation and smoke control in underground car parks?
- What is the significance of utilizing fire-resistant materials and components in jet fans to ensure their operational durability during fire events?

This study makes a substantial contribution to the existing knowledge landscape by shedding new light on the effectiveness of jet fan ventilation systems within expansive underground car parks, meticulously aligning with contemporary legislative frameworks. Going beyond the confines of prior research, it rigorously examines the nuanced dynamics of visibility distribution—an often-underestimated factor that profoundly impacts both the efficacy of evacuation procedures and the intricacies of fire extinguishing protocols.

Moreover, in emphasizing the pivotal role of fire resistance in fan units, this research highlights the critical need for these components to exhibit formidable resilience against elevated temperatures during fire-related scenarios, ensuring a robust line of defense in the event of emergencies. In addition to these pivotal insights, the practical recommendations advanced within this paper serve as an indispensable roadmap for professionals spanning the domains of architecture, construction, and ventilation engineering. By offering nuanced guidelines for optimal fan placement and precision-driven speed configurations, this study actively equips practitioners with the tools to elevate the overall health, safety, and operational efficiency of underground car park facilities.

2. Materials and Methods

This section presents the methodology employed for the current study, as depicted in Figure 1. The simulations are carried out in two distinct phases utilizing OpenFOAM v1806, a widely recognized open-source computational fluid dynamics (CFD) software built on the C++ programming language. In Phase 01, the velocity fields are obtained, while Phase

02 focuses on modeling the propagation of smoke within the fully developed velocity fields. In total, over 40 simulations are run, with each taking more than 40 h, using a workstation with a CPU: AMD 3990X − 64 × 2.9 GHz, cache: 256 MB, RAM: 64 GB, and graphics card: 24 GB (2 × 32 GB). The obtained results are subsequently post-processed using Paraview, an open-source, cross-platform application designed for interactive scientific visualization.

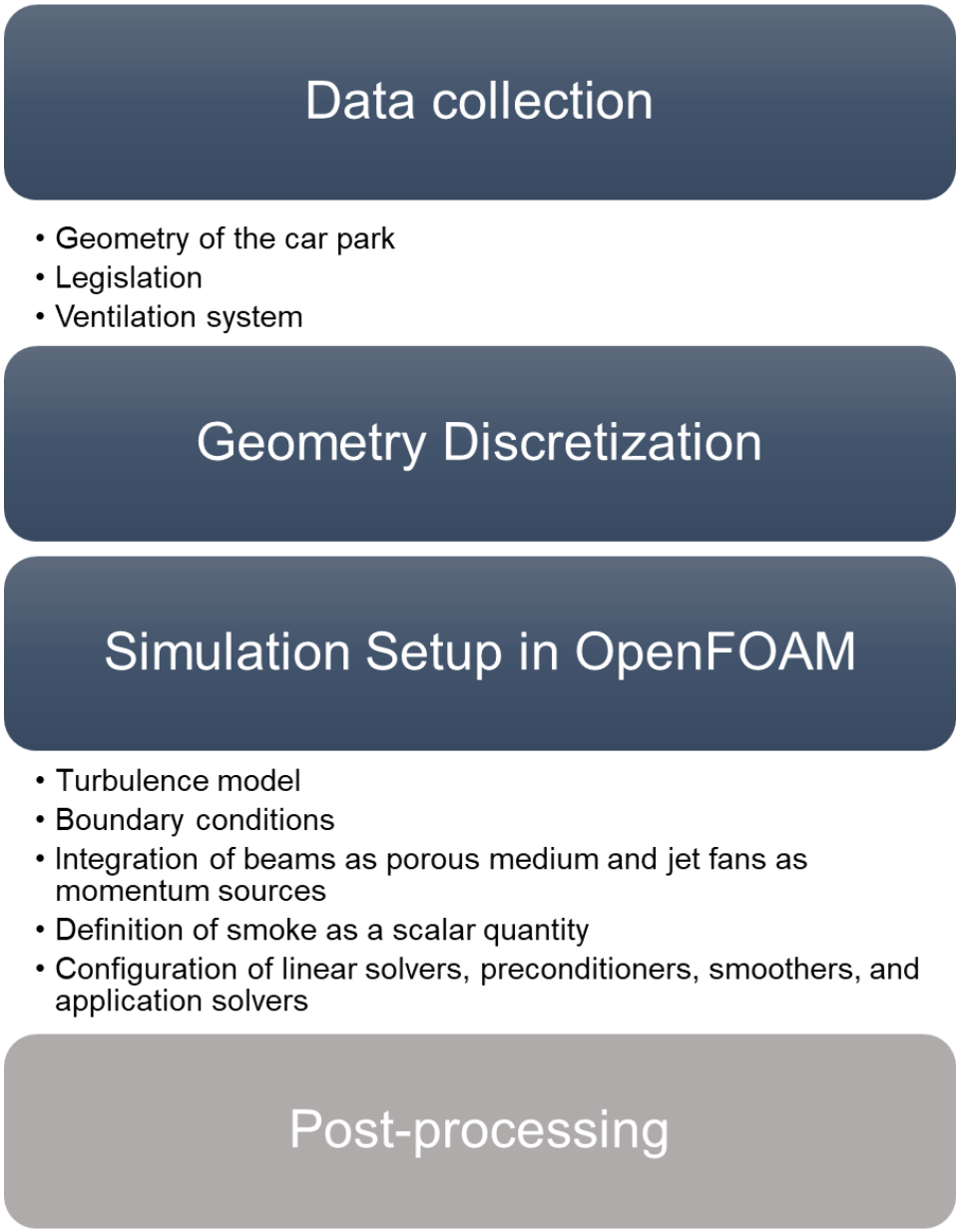

Figure 1. Hierarchy of the method.

2.1. Data Collection

2.1.1. Geometry of the Car Park

This thesis work focuses on a case study of a mall car park located in Tabriz, Iran, with a total area of approximately 21,670 m^2. The capacity of the car park is 450 vehicles. The enclosed area has a height of 3 m. The car park is divided into four separate zones, as illustrated in Figure 2. Each subdivision of the car park has the following resulting areas:

- Zone 1: 5900 m^2.
- Zone 2: 5120 m^2.
- Zone 3: 5030 m^2.

- Zone 4: 5620 m^2.

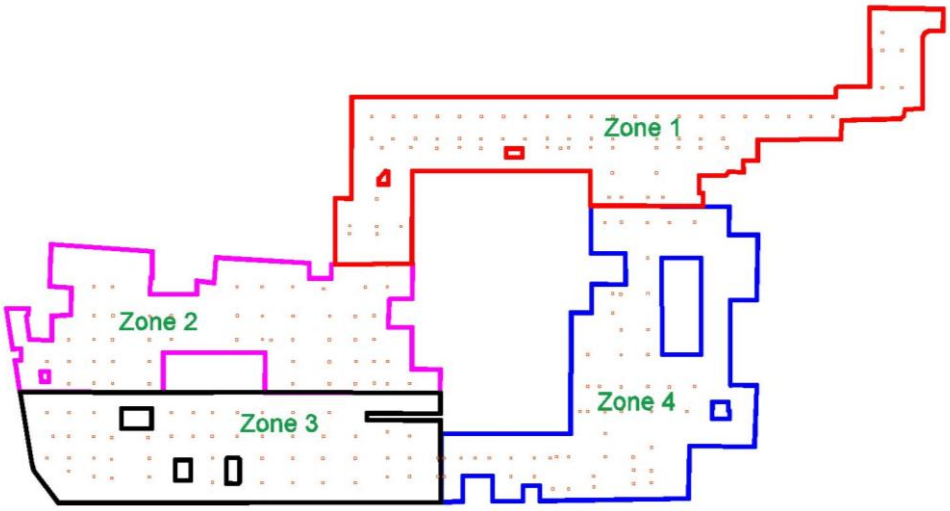

Figure 2. Division of car park area into four distinct zones.

2.1.2. Legislation

The legislation widely adopted for car park ventilation in the studied region includes the approved documents F and B, issued by the Ministry of Housing, Communities, and Local Government of the UK. Approved document F [24] establishes air quality and ventilation standards for various types of buildings under normal conditions. For enclosed areas, like car parks, it specifies that the average concentration of harmful components, particularly CO, should not exceed 30 ppm over an eight-hour period. Additionally, the maximum concentration in exits, entrances, and ramps where cars are in motion or parked with running engines should not exceed 90 ppm. The document recommends 6 air changes per hour for the entire car park and 10 air changes per hour for exits, entrances, and ramps.

Approved document B [25] addresses fire safety standards. It stipulates that the fire load must be defined, and if the design is satisfactory for a specific floor, the potential spread of fire to other levels should be minimal. In the event of a fire, the ventilation system should be capable of providing 10 air changes per hour. Moreover, the system should be designed in two equal parts, each capable of functioning independently or simultaneously.

2.1.3. Ventilation System

The study utilized a ventilation system comprising both jet fans and axial fans. Jet fans are responsible for generating a forceful stream of compressed air, effectively propelling the air forward. These jet fans are strategically placed throughout various zones to facilitate the movement of air from the supply points to the exhaust points. Due to their compact design, jet fans are particularly suitable for enclosed spaces with limited vertical clearance. Table 2 provides an overview of the specific features of the jet fans selected for this study.

Table 2. Characteristics of jet fans (derived from manufacturer's data).

Performance Index	Air Flow [m^3/s]	Air Speed [m/s]	Thrust [N]
Value	2.88/1.44	22.3/11.2	78/20

The axial fans are designed to deliver large volumes of low-pressure air, suitable for both air supply and exhaust purposes. Each zone requires two exhaust shafts and two supply fans, which can be operated independently or simultaneously. Each fan set is designed to provide 50% of the total ventilation capacity required for the zone, following

the guidelines outlined in approved document B. To calculate the ventilation capacity of each supply and exhaust shaft, the following formula can be utilized:

$$DAF_i = \frac{V_i \times n}{2 \times 3600} \quad (1)$$

where DAF_i is the design air flow rate of each supply/exhaust shaft of the zone i, V [m^3] is the total volume of the zone i, and n [ach] is the number of required air changes per hour. To ensure consistency across all four zones, it is assumed that the supply/exhaust shafts are identical. The required design flow rate for each fan is calculated based on the highest volume, which is found in Zone 1 and measures 17,700 m^3. Employing Equation (1), the design flow rate for each fan is determined to be 22.5 m^3/s. This calculation allows for the appropriate sizing and specification of the fans to effectively meet the airflow requirements of the zones.

2.2. Discretization Process

Figure 3 illustrates the utilization of Pointwise 18.2 software, which is a well-established and robust computational fluid dynamics (CFD) meshing tool renowned for its capability to generate high-quality and well-structured meshes [26]. The study implements a 3D structured mesh composed of hexahedral Cartesian elements. Despite the challenges inherent in dealing with large and complex geometries, the deliberate selection of a structured mesh over an unstructured alternative is motivated by a range of significant advantages, such as enhanced control and precision, improved convergence properties, access to supplementary solution algorithms, effective resolution of data locality issues, and the ability to define normal vectors [27]. A total of 173,332,000 nodes and 7,222,200 units were generated by the fluid grid division.

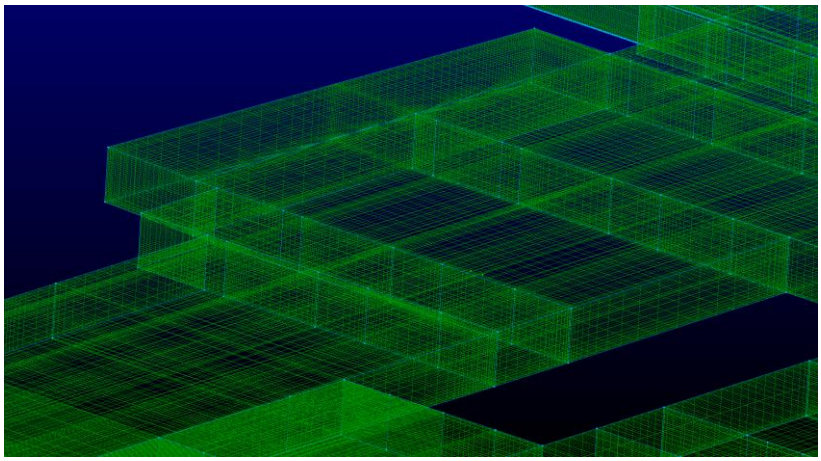

Figure 3. An enlarged portion of the mesh, providing improved resolution and detailed visualization.

In an OpenFOAM CFD simulation employing a Cartesian grid, a variety of parameters can be calculated using the finite volume method. This involves transforming the governing equations from their continuous formulation to integral forms across each volume, which includes the process of averaging the equations over the respective volume. These governing equations pertain to the discretization of partial differential equations (PDEs) within the Cartesian coordinate system, and the parameters under consideration encompass fundamental physical properties, such as velocity, pressure, temperature, and more. For incompressible flow without any source or sink terms, the corresponding continuous

form of continuity equations (mass conservation—Equation (2)) and momentum equations (Navier–Stokes equations—Equation (3)) are as follows [28]:

$$\frac{\partial \rho}{\partial t} + \frac{\partial(\rho u)}{\partial x} + \frac{\partial(\rho v)}{\partial y} + \frac{\partial(\rho w)}{\partial z} = 0 \tag{2}$$

$$\frac{\partial(\rho u)}{\partial t} + \frac{\partial(\rho uu)}{\partial x} + \frac{\partial(\rho vu)}{\partial y} + \frac{\partial(\rho wu)}{\partial z} = -\frac{\partial p}{\partial x} + \mu\left(\frac{\partial^2 u}{\partial x^2} + \frac{\partial^2 u}{\partial y^2} + \frac{\partial^2 u}{\partial z^2}\right) + \rho g_x \tag{3}$$

$$\frac{\partial(\rho v)}{\partial t} + \frac{\partial(\rho v)}{\partial x} + \frac{\partial(\rho vv)}{\partial y} + \frac{\partial(\rho wv)}{\partial z} = -\frac{\partial p}{\partial y} + \mu\left(\frac{\partial^2 v}{\partial x^2} + \frac{\partial^2 v}{\partial y^2} + \frac{\partial^2 v}{\partial z^2}\right) + \rho g_y$$

$$\frac{\partial(\rho w)}{\partial t} + \frac{\partial(\rho uw)}{\partial x} + \frac{\partial(\rho vw)}{\partial y} + \frac{\partial(\rho ww)}{\partial z} = -\frac{\partial p}{\partial z} + \mu\left(\frac{\partial^2 w}{\partial x^2} + \frac{\partial^2 w}{\partial y^2} + \frac{\partial^2 w}{\partial z^2}\right) + \rho g_z$$

where ρ is density [kg/m^3], u, v, and w are velocity components in the x, y, and z directions [m/s], p is pressure [Pa], μ is dynamic viscosity [Pa·s], and g_x, g_y, and g_z are acceleration due to gravity in the x, y, and z directions [m/s^2]. The continuity equation asserts that the alteration in mass within a control volume must be offset by the mass movement across its boundaries. In simpler terms, the total mass fluxes along the x, y, and z axes should sum up to zero, ensuring mass continuity. Conversely, the momentum equations illustrate how momentum changes in each direction due to certain factors, like convection, pressure gradients, viscosity, and gravity.

2.3. Simulation Setup in OpenFOAM

2.3.1. Turbulence Model

The selection of a turbulence model for CFD analysis plays a critical role in accurately simulating fluid flows. Turbulence models allow for accounting for the turbulent nature of flows, which is pervasive in many fluid dynamics scenarios. In the realm of CFD, several turbulence models are available, including Reynolds-averaged Navier–Stokes (RANS), large eddy simulations (LES), unsteady RANS (URANS), hybrid RANS–LES, and direct numerical simulation (DNS). Each model comes with its own computational cost and level of accuracy. In the context of this study, the $k-\varepsilon$ turbulence model, belonging to the RANS family, is chosen, as it is widely employed in indoor environment simulations [29]. It consists of two transport equations for turbulent kinetic energy (k) [m^{2}s^{-2}] and turbulence dissipation rate (ε) [m^{2}s^{-3}]. The k equation is as follows [30]:

$$\frac{D}{Dt}(\rho k) = \nabla\cdot(\rho D_k \nabla k) + P - \rho\varepsilon \tag{4}$$

where D_k is the effective diffusivity for k [-], and P is the turbulent kinetic energy production rate [m^{2}s^{-3}]. The ε equation is as follows [30]:

$$\frac{D}{Dt}(\rho\varepsilon) = \nabla\cdot(\rho D_\varepsilon \nabla\varepsilon) + \frac{C_1\varepsilon}{k}\left(P + C_3\frac{2}{3}k\nabla\cdot u\right) - C_2\rho\frac{\varepsilon^2}{k} \tag{5}$$

where D_ε is effective diffusivity for ε [-], C_1 and C_2 are model coefficient [-]. The $k-\varepsilon$ turbulence model is robust and reduces the memory needed for the analysis while maintaining reasonable accuracy. This model assumes the flow to be fully turbulent, disregarding the molecular viscosity. The adoption of the $k-\varepsilon$ turbulence model is justified by its favorable balance between computational efficiency and accuracy, aligning well with the study's focus on initial monitoring and iterative investigations. This choice optimizes resources for timely insights into dominant turbulent flow behavior, while acknowledging the model's limitations in pressure gradients and streamline curvature [31]. Top of Form.

2.3.2. Boundary Conditions

In the context of CFD analysis, boundary conditions refer to specific regions that exhibit distinct flow behavior, which is described by a predefined set of parameters based on the selected turbulence model. This study focuses on defining boundary conditions using the $k - \varepsilon$ model, where initial values for pressure (p), velocity (U), turbulent kinetic energy (k), and rate of dissipation of turbulent kinetic energy (ϵ) need to be specified. Three different types of boundary conditions are considered: inlet/outlet (representing supply/exhaust shafts), parking entrance, and wall surfaces. The characteristics of these boundary conditions are summarized in Table 3.

Table 3. Definition of boundary conditions in OpenFOAM.

Boundary	p [Pa]	U [m/s]	K [m^2s^{-2}]	ε [m^2s^{-3}]
Inlet/outlet (supply/exhaust shafts)	Type: fanPressure—patchType: total Pressure—file: fanCurve—direction: in (supply) or out (exhaust)—$p0$: uniform 0	pressureInletOutletVeloicity—value: uniform (0,0,0)	fixedValue—value: $internalField: uniform 0.375	fixedValue—value: $internalField: uniform 14.855
Parking entrance	fixedValue—value: uniform 0	zeroGradient–$\frac{\partial U}{\partial n} = 0$	zeroGradient–$\frac{\partial k}{\partial n} = 0$	zeroGradient–$\frac{\partial \varepsilon}{\partial n} = 0$
Walls	zeroGradient–$\frac{\partial p}{\partial n} = 0$	fixedValue—value: uniform (0,0,0)	kqRWallFunction—value: $internalField: uniform 0.375	epsilonWallFunction—value: $internalField: uniform 14.855

Within the OpenFOAM simulation, the gas–solid interface (in wall boundary conditions) is defined by carefully crafted wall conditions that encompass a spectrum of physical phenomena, including elements, such as viscous shear, pressure gradients, and thermal effects. These dynamic wall conditions actively shape the gas flow patterns in proximity to solid surfaces, ensuring an accurate replication of the intricate details of the interaction. Moreover, the chosen RANS turbulence model equations adeptly capture the complex flow dynamics taking place in the vicinity of the gas–solid interface. This RANS model takes into account the intricate processes of turbulence eddy generation and dissipation, serving as a pivotal mechanism for facilitating the exchange of momentum and energy between the gas and solid phases.

It is important to note that the pressure (p) boundary condition applied to the inlet/outlet shafts is based on data stored in the "file: fanCurve" directory. This data encompasses flux values for the fan across different static pressures, extracted from the manufacturer's provided fan characteristics curve and listed in Table 4.

Table 4. Flux and static pressure values for inlet/outlet axial fans obtained from manufacturer-provided data.

Static Pressure [Pa]	0	50	100	150	200	250	300	400	500	600
Flux [m^3/s]	22.3	21.9	21.39	20.86	20.31	19.75	19.17	17.9	16.45	14.6

2.3.3. Integration of Beams as Porous Medium and Jet Fans as Momentum Sources

A simplified approach is utilized to assess the effect of multiple beams distributed throughout the parking area. In this approach, the beams are treated as porous mediums with an infinite pressure gradient, effectively functioning as solid walls without air penetration. The modeling technique employed for this purpose is the Darcy–Forchheimer porous medium model. According to this model, the flow rate (Q) of any fluid into the porous medium bed is directly proportional to the filter area (A) and the difference in fluid head

between the inlet and outlet of the medium (Δh), while being inversely proportional to the thickness of the bed (L), as follows [32]:

$$Q = \frac{C \times A \times \Delta h}{L} \tag{6}$$

The Darcy–Forchheimer model [33] works as a sink in the momentum equation. To implement the beams as porous media, the elements confined by the beams (or beam coordinates) must be defined in the topoSet dictionary and adjusted in the porousityProperties dictionary in OpenFOAM.

In contrast, the induction fans in this study are defined as momentum sources. These momentum sources introduce a source term in the momentum equations that acts in the opposite direction to the porous media. To incorporate the induction fans into the simulation, the corresponding cellZones must be defined in the topoSet dictionary. Subsequently, all necessary adjustments will be made in the fvOptions dictionary. The velocity of the momentum sources is assumed to be 22.3/11.2 m/s, based on the specifications provided for the jet fans (see Section 2.1.3).

2.3.4. Definition of Smoke as a Scalar Quantity

In this study, the smoke concentration produced by a fire is defined as a scalar quantity. In OpenFOAM, a scalar quantity refers to a physical quantity that has magnitude but does not have a specific direction associated with it. It represents a single value at each point in a computational domain. Examples of scalar quantities in OpenFOAM include pressure, temperature, concentration, and turbulence kinetic energy. The smoke concentration production rate $\dot{m}_s$ [kg/m^{3}s] can be calculated as follows:

$$\dot{m}_s = \dot{M}_s / V_s \tag{7}$$

where $\dot{M}_s$ represents the rate at which smoke mass is produced and V_s indicates the volume of the smoke source. According to [34], fire events and incidents involving vehicles estimate a burning rate of 260 kw/m^2 for a fire area of 6 m^2, which is equivalent to burning 145 kg of wood. The rate of fuel mass consumption, denoted as $\dot{m}_f$, is estimated to be 0.61 kg/s [35]. To calculate the production rate of smoke concentration, the fuel mass rate can be converted using the yield factor y_p [34], as follows:

$$\dot{M}_s = y_p \, \dot{m}_f = 0.61 \times 0.018 = 0.01098 \ [\text{kg/s}] \tag{8}$$

According to the recommendations in [36], for an indoor car park without a sprinkler system, the suggested dimensions for the fire source area are 5 m × 5 m. Based on experimental data in [35], the height of the resulting smoke source from a car fire is measured to be 0.8 m. Therefore, the volume of the smoke source V_s can be calculated as 5 m × 5 m × 0.8 m. By utilizing Formula (3), the rate of mass concentration production is determined to be 5.49×10^{-4} kg/m^{3}s. This value is then assigned as the smoke source intensity within the fvOptions dictionary, specifically for a cellZone with a boxed shape in the topoSet dictionary.

2.3.5. Configuration of Linear Solvers, Preconditioners, Smoothers, and Application Solvers

In this section, all the configurations for the linear solvers, preconditioners, smoothers, and application solvers for two phases (Phase 01 and Phase 02) of the simulations are specified.

Linear Solvers

In OpenFOAM, the discretized equations in the simulation are solved using linear solvers. It is important to note that the term "*linear solver*" refers to the method used to

solve a set of linear equations, while the "*application solver*" describes the set of equations and algorithms used to solve a specific problem.

During Phase 01, the generalized geometric–algebraic multigrid (GAMG) method is employed as the linear solver to calculate the pressure field p. The multigrid linear solvers utilize a coarse grid with fast solution times to generate an initial solution for the fine grid, effectively reducing errors with high frequency. GAMG utilizes either a geometric or algebraic pairing agglomeration procedure, gradually coarsening the mesh [37]. GAMG is suitable for complex geometries and delivers accurate solutions for the pressure field. To calculate other properties, such as U, ε, and k, the smoothSolver is used in an iterative manner. This solver employs a chosen smoother at runtime to solve symmetric and asymmetric matrices. For Phase 02, the preconditioned bi-conjugate gradient (PBiCGStab) linear solver is selected due to its favorable parallel scaling and efficient utilization of computational resources. As Phase 02 involves modeling the propagation of smoke as a scalar quantity T, which typically entails solving asymmetric matrices, the PBiCGStab solver is well-suited for this task. These configurations pertaining to the linear solvers are adjusted in the fvSolution dictionary.

Preconditioners

Preconditioners play a crucial role in improving the convergence speed of linear equation solvers compared to the original equations [37]. In Phase 01, when calculating pressure field p, the diagonal-based incomplete Cholesky (DIC) preconditioner is employed. This preconditioner involves reorganizing the linear equations and computing the reciprocal diagonal matrix, which is then determined and stored for symmetric matrices. To derive the smoke concentration T in Phase 02, and for the calculation of other properties, such as U, ε, and k in Phase 01, the diagonal-based incomplete LU (DILU) preconditioner is utilized. DILU is similar to DIC, but it is specifically designed for handling asymmetric matrices. These configurations pertaining to the preconditioners are adjusted in the fvSolution dictionary.

Smoothers

Preconditioners are utilized to reduce the number of iterations required to solve linear equations, but they do not directly impact the number of iterations associated with mesh-related calculations. To address this issue, smoothers are employed in conjunction with solvers. Smoothers play a role in modifying the mesh shape while preserving its topology, leading to improved quality of the volume mesh. During Phase 01, for all properties of the flow field, the Gauss–Seidel method is selected as the smoother. This choice is motivated by the large number of meshing elements. The Gauss–Seidel method is known for its cost-effectiveness in terms of memory usage. It is an iterative method that aims to solve algebraic equations by iteratively approaching the desired accuracy with an approximate solution. However, it should be noted that smoothers are not implemented during the simulations in Phase 02. These configurations regarding the smoothers are adjusted in the fvSolution dictionary, ensuring their appropriate settings for the simulations.

Application Solvers

As mentioned earlier, the "application solver" refers to the set of equations and algorithms employed to solve specific problems. In incompressible flows, the coupling between pressure and velocity poses challenges when determining the velocity field using Navier–Stokes equations. This difficulty arises because pressure is not a primary variable in the momentum or continuity equations [38]. To address this, the semi-implicit method for pressure-linked equations (SIMPLE) algorithm is introduced in [39]. This algorithm iteratively develops the velocity and pressure fields, ensuring the validation of the momentum and continuity equations. The solution is reached when both equations are satisfied during each iteration. This approach is known as a segregated approach, as it sequentially resolves the velocity and pressure fields instead of simultaneously solving them [38,40]. In Phase 01

of the simulations, the porousSimpleFoam solver is chosen to account for beams modeled as porous media with a significant pressure drop.

For Phase 02, the scalarTransportFoam solver is utilized as the application solver. scalarTransportFoam is a fundamental solver available in OpenFOAM, designed to solve transport equations for passive scalars using a predefined constant velocity field. It is commonly used for diffusion–convection problems, involving the transport of scalars without any source term.

All the configurations for the linear solvers, preconditioners, smoothers, and application solvers are summarized in Table 5.

Table 5. Configuration of linear solvers, preconditioners, smoothers, and application solvers for Phase 01 and Phase 02.

	Phase 01	**Phase 02**
Linear solver	p: GAMG U, ε, and k: smoothSolver	T: PBiCGStab
Preconditioner	p: DIC U, ε, and k: DILU	T: DILU
Smoother	GaussSeidel	-
Application solver	porousSimpleFoam	scalarTransportFoam

3. Results

This section is dedicated to presenting the study's outcomes. It should be mentioned that the parameter governing convergence is established through the "residualControl," a constituent of the solver settings enabling specification of convergence criteria for various variables (or fields) within the simulation. This mechanism defines the tolerable extent of disparity (residual) between discretized equations and their resolved counterparts. The solver deems the simulation converged and concludes its iterations when residuals for all designated fields dip below stipulated convergence criteria. For this study, the convergence criterion for all parameters (p, U, k, and ε) is uniformly set at 1×10^{-6}, while a consistent time interval of one second is implemented across all simulations.

Figure 4 (left) showcases the results of simulations for the base case placement of jet fans. These jet fans are assumed to operate in high-speed mode, generating an outlet air velocity of 22.3 m/s. As illustrated in Figure 4 (right), this design yields satisfactory airflow from the supply to the exhaust points. However, certain areas in zones 1, 3, and 4 experience stagnation points where the airflow nearly ceases, posing a risk of smoke concentration in those regions. It is important to note that all subsequent visualizations represent slices taken at a height of 1.7 m, which is considered the average human height.

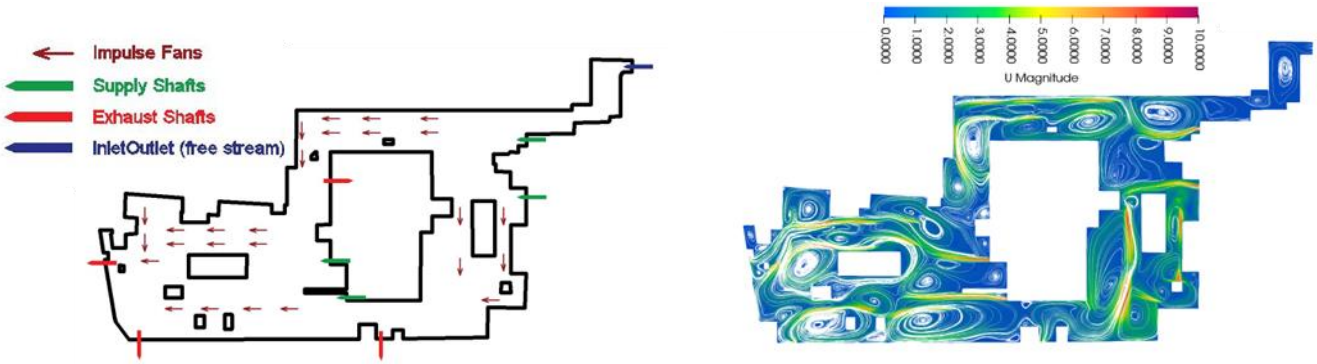

Figure 4. Base case jet fan positioning (**left**) and resulting velocity field (**right**).

In order to examine the impact of fire source location, a total of 17 distinct scenarios were investigated. The fire scenarios were determined by starting from the initial location and extending 30 m in all directions. However, due to computational constraints, certain

fire locations had to be omitted from the study. Figure 5 depicts the 17 selected fire source location scenarios, providing a visual representation of the varied positions considered.

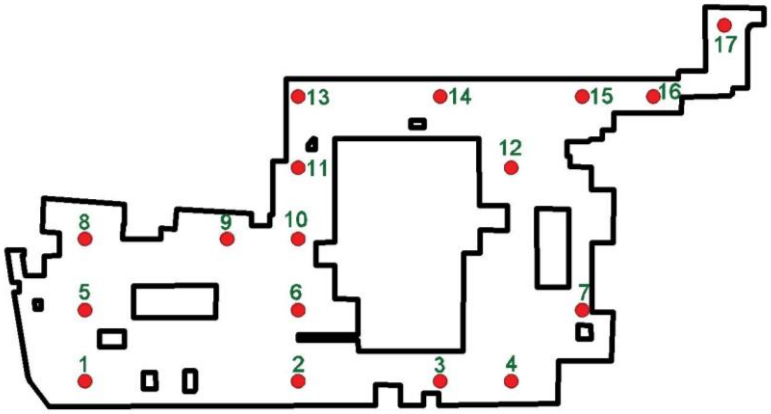

Figure 5. Scenarios for fire location. Each scenario represents a distinct fire location, demonstrating the potential spread and impact of smoke in the studied area.

To analyze the propagation of smoke and determine the visibility distribution within the car park, the calculator provided in Paraview is utilized to convert the rate of smoke concentration $\dot{m}_s$ to visibility S [34] using the following formula:

$$S = K/\alpha_m \dot{m}_s \tag{9}$$

where K is proportionally constant for the visibility for different illumination scenarios as shown in Table 6, and α_m is the specific extinction coefficient for different modes of combustion, as shown in Table 7. Given the presence of illuminated signs in the car park to aid in the evacuation process, a proportional constant of $K = 8$ is applied. Considering the initial stages of a car fire, which primarily involve flaming combustion, it is justifiable to assign an extinction coefficient of $\alpha_m = 7875.2$. This post-processing analysis using Paraview's calculator provides a quantitative understanding of how the smoke propagates and affects visibility within the car park. It enables the assessment of potential visibility hazards in different areas, aiding in the identification of high-risk zones and informing appropriate safety measures and evacuation protocols.

Table 6. Proportional constants for different illumination scenarios [34].

Situation	K
Building components in reflected light	3
Illuminated signs	8
Reflecting signs	3

Table 7. Extinction coefficients for different modes of combustion [34].

Mode of Combustion	α_m $[\frac{m^2}{kg}]$
Flaming combustion	7875.2
Smoldering combustion	4301.1

Figure 6 illustrates the distribution of visibility for the eight worst-case scenarios (i.e., scenarios 2, 4, 7, 9, 11, 13, 14, and 15), presenting a visual representation of how visibility is affected in each scenario. Appendix A contains the remaining figures for further exploration. Contours are set to the value of 10 m in all visibility fields to show the capability of the ventilation system in maintaining a clear path for the firefighters to reach to the firebase by 10 m.

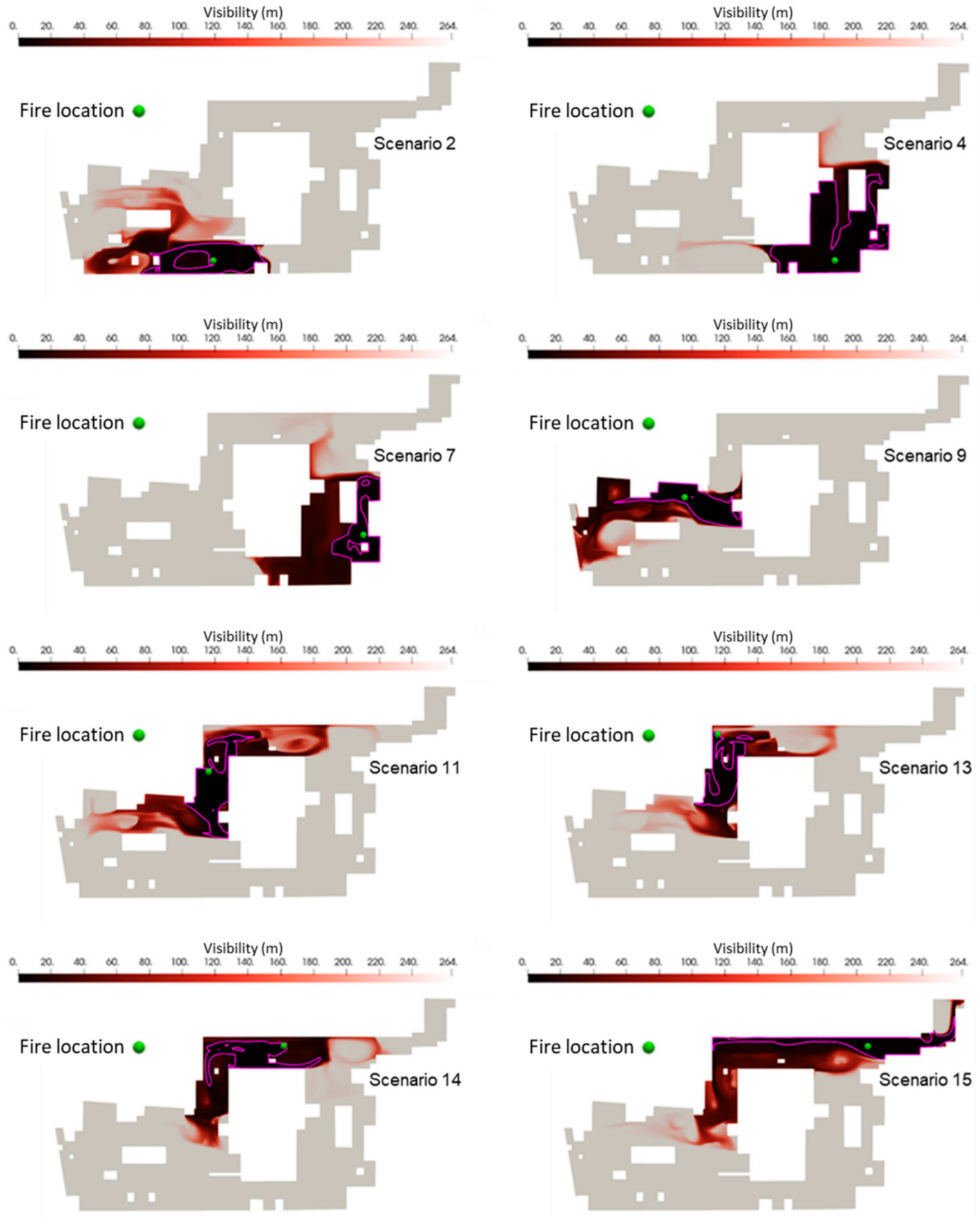

Figure 6. Visibility distribution for the base case jet fan positioning for different fire location scenarios.

Based on the visibility results, it is evident that the base case jet fan positioning is inadequate for effectively removing the smoke generated, particularly in Zone 4. Additionally, in both Scenario 2 and Scenario 15, the presence of smoke hinders firefighters from approaching the fire source due to a limited visibility of 10 m. Moreover, the smoke dispersion towards the parking entrance in Scenario 15 not only obstructs access but also prevents firefighters from entering the parking area altogether. These observations highlight significant challenges posed by the smoke propagation within the car park during fire incidents. The insufficient ventilation system, coupled with the smoke's adverse effects on visibility, impedes the critical tasks of firefighting and evacuation.

These findings underscore the significance of reevaluating and enhancing the ventilation system design to optimize smoke extraction efficiency and overcome the challenges that firefighters encounter when approaching the fire source. Consequently, a new positioning for the jet fans is proposed, as depicted in Figure 7 (left), with the aim of improving ventilation in Zone 4 and minimizing the presence of extensive recirculating flows in Zone 1 and Zone 3. In the proposed configuration, ten new jet fans are incorporated, and low-speed jet fans are considered, generating an outlet air velocity of 11.2 m/s. In addition, the exhaust shaft is moved closer to the supply shaft in Zone 4. This results in a new velocity field, as illustrated in Figure 7 (right). This revised setup seeks to achieve more effective airflow patterns, facilitating the removal of smoke from critical areas within the car park. Figure 8 displays the visibility distributions corresponding to various fire source locations for the suggested fan configuration.

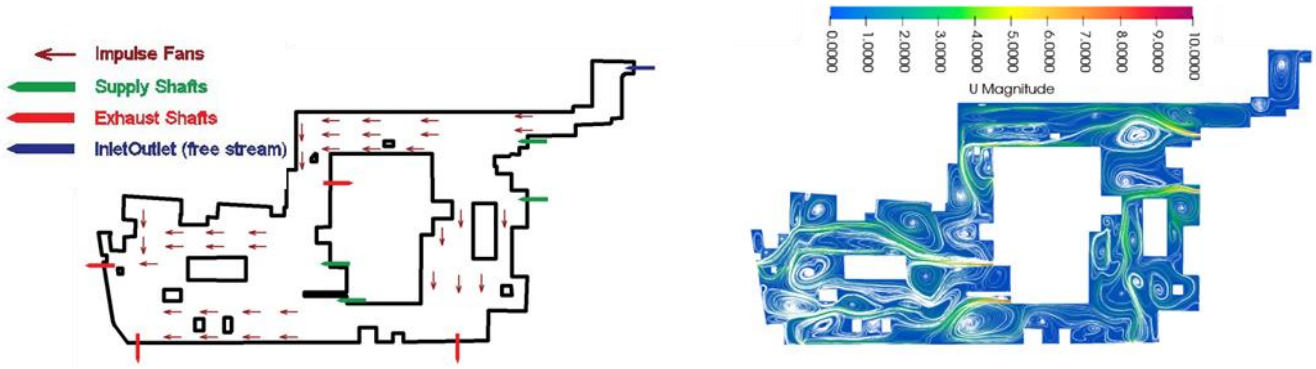

Figure 7. Proposed fan positioning (**left**) and resulting velocity field (**right**).

The enhanced ventilation system configuration clearly demonstrates an improved capability in effectively removing smoke during fire events. Notably, a comparison between scenarios 1, 2, 4, 7, 9, and 15 (see also Appendix A) in both the base case and proposed fan setups reveals the significant improvement achieved in ventilation. Although there is an increase in smoke dispersion in scenarios 9, 14, 18, 19, and 24, the primary objective of the study, which is to ensure smoke clearance while maintaining visibility above 10 m from the fire source, has been successfully met. This objective was previously compromised in the base case fan setup in scenarios 2, 4, 7, and 15.

To conduct a more detailed analysis of fire Scenario 2, which is considered the most challenging in terms of smoke dispersion, further investigations are carried out for the proposed fan setup. In this analysis, it is assumed that two jet fans adjacent to the fire source become non-operational due to excessive heat, as depicted in Figure 9. By replicating the simulations under these specific conditions, the resulting visibility field is obtained and presented in Figure 10. The findings clearly demonstrate that the smoke dispersion is significantly extended towards Zone 4, indicating the potential risks associated with impaired jet fan operation during fire incidents. This outcome highlights the critical importance of utilizing fire-resistant fans equipped with fireproof electromotors and ensuring their regular maintenance. By employing such measures, the operation of jet fans can be ensured even under extreme circumstances.

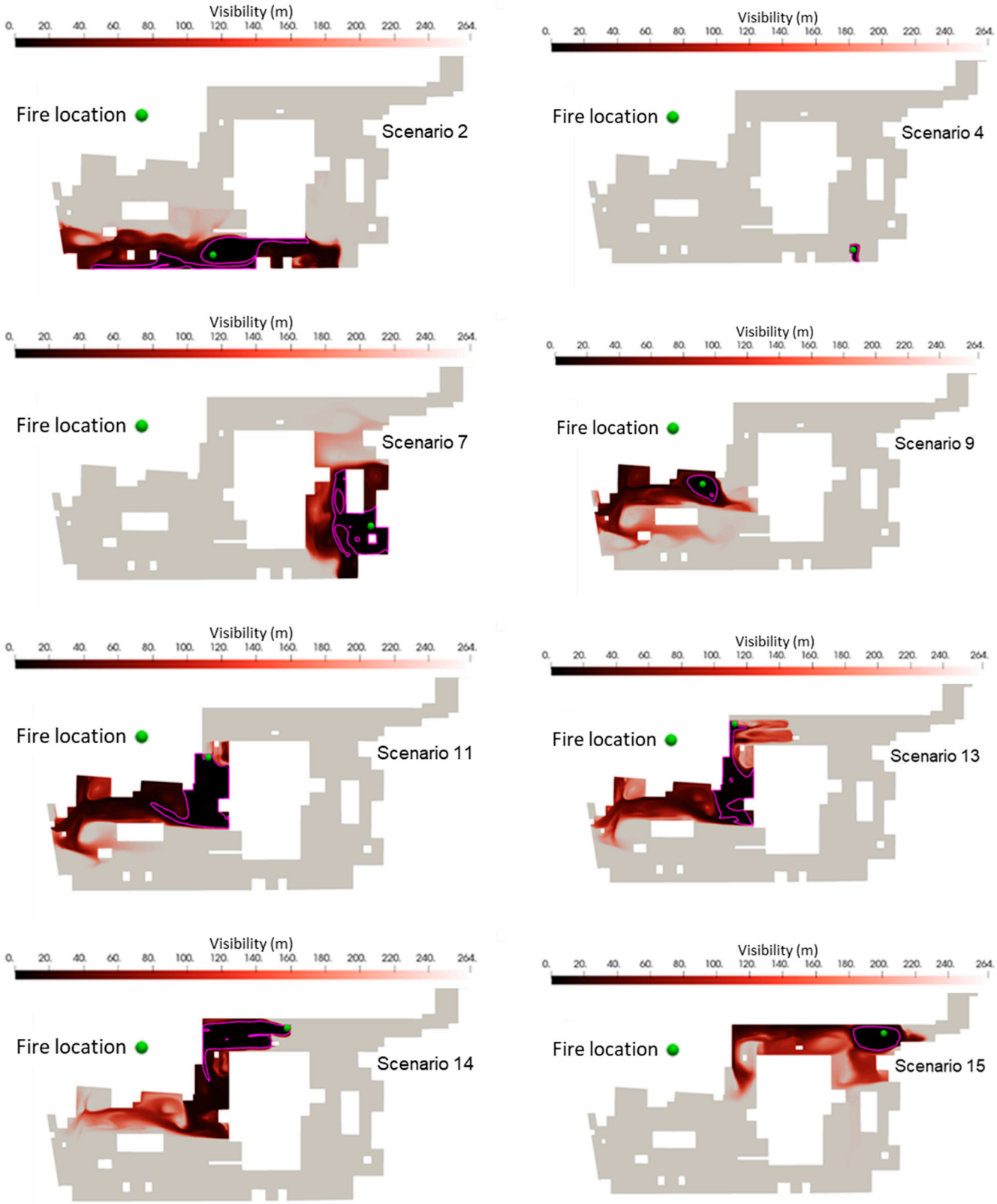

Figure 8. Visibility distribution for the proposed fan positioning for different fire location scenarios.

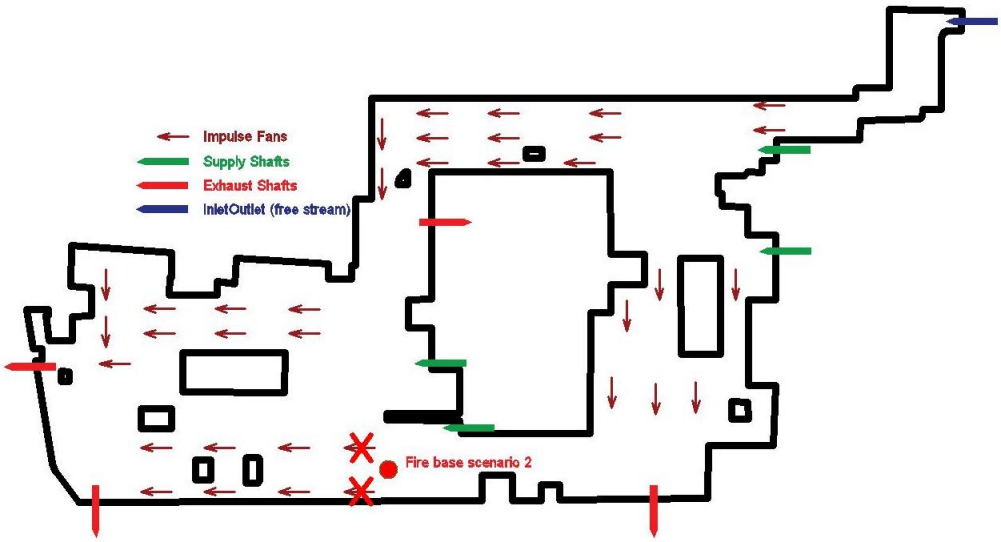

Figure 9. Illustration of the jet fans' operational status, with specific emphasis on the scenario where two fans adjacent to the fire source in Scenario 2 are non-operational.

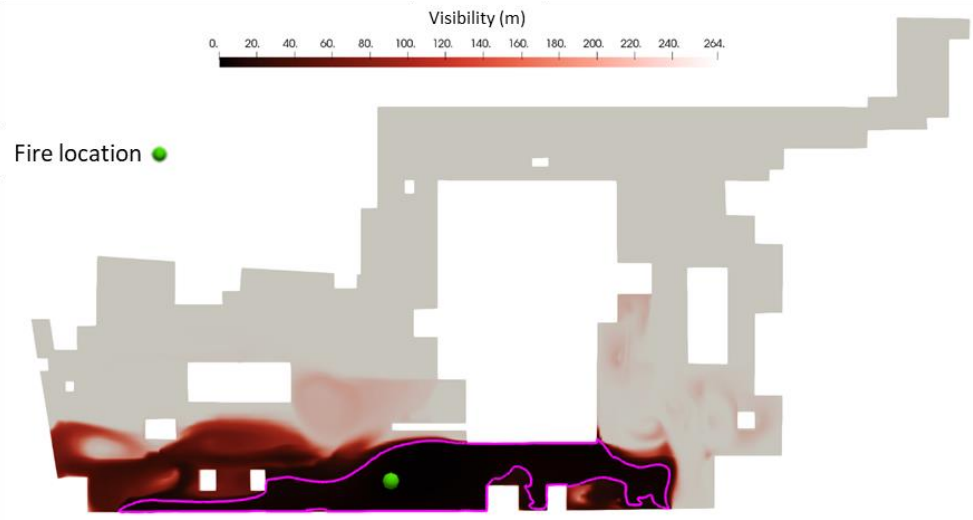

Figure 10. Visibility distribution for the proposed fan positioning, when two fans adjacent to the fire source in Scenario 2 are non-operational.

4. Discussion and Conclusions

The simulations conducted using OpenFOAM provide valuable insights into the behavior of the jet fan system in controlling smoke dispersion caused by car fires within enclosed areas. The analysis involves deriving velocity fields and evaluating visibility conditions to understand the efficiency and effectiveness of the system. The main findings of the study can be summarized as follows:

- Jet fan positioning and back-layering: The positioning of the jet fan system components significantly impacts its efficiency. Jet fans placed near the ceiling create a jet among themselves, necessitating the use of multiple lines of jet fans to prevent back-layering. Back-layering refers to "*Movement of smoke and hot gasses counter to the direction of the ventilation airflow*" according to National Fire Protection Association NFPA, which can reduce the ventilation efficiency. In the proposed design in this study, adding 10 extra jet fans to form additional lines in Zone 1 and Zone 3 enhances the capability of the ventilation system to prevent lateral smoke dispersion.
- Jet fan air flow rate: The analysis of air flow rates shows when jet fans direct an excessive airflow towards the exhaust shafts (which have a designated flow rate of

22.5 m^3/s), recirculating flows occur, leading to the dispersion of smoke throughout the car park. Consequently, the utilization of low-velocity jet fans (11.2 m/s) proves to be more effective in clearing smoke compared to high-velocity jet fans (22.3 m/s).

- Optimal positioning of supply and exhaust shafts: Achieving optimal smoke control involves positioning the supply and exhaust shafts on opposite walls or minimizing the number of air flow turns between the supply and exhaust points. Ideally, all outlets should be placed directly opposite the inlets throughout the design, ensuring efficient ventilation and smoke control. In the proposed design, for instance, placing the exhaust shafts closer to the supply shaft in Zone 4 results in reduced back-layering compared to the same zone in the base case.
- Fire resistance of jet fans: It is crucial for the jet fans utilized in the system to possess fire resistance capabilities, enabling them to continue operating for a certain duration during fire events. The study underscores the significance of utilizing fire-resistant materials and components in jet fans, as their failure can result in severe conditions.
- Future research is recommended in the following directions:
- In order to further validate the findings of this study, it is recommended that future research incorporates experimental studies. By combining computational simulations with real-world experimentation, this approach will provide stronger evidence and enhance the credibility of the study's findings.
- To gain a deeper understanding of the effectiveness of jet fan ventilation systems, future research should compare their performance with conventional systems, such as ventilation through ducts. This comparative analysis will offer insights into the advantages and limitations of each approach.
- Future research is recommended to conduct sensitivity analysis on key properties of jet fans and supply/exhaust shafts, such as air flow rate, air velocity, thrust, etc. By systematically varying these parameters, researchers can identify their impact on system performance and optimize their values accordingly.
- Future research should focus on investigating optimal jet fan positioning, aiming to provide practical guidelines that are solid and robust. This would enable engineers and practitioners to implement jet fan systems with confidence, knowing they are following the most effective and efficient layout.
- To enhance the operational efficiency of jet fan ventilation systems, future research should explore the integration of advanced control strategies, such as real-time feedback mechanisms or predictive modeling. Further investigations in this context can yield valuable insights into optimizing fan operation for improved smoke dispersion and evacuation efficiency.
- For future research, it is advisable to embark on a multi-physics analysis that combines simulations encompassing thermal dynamics, structural response, and fire propagation. This integration of distinct disciplines results in a thorough and all-encompassing safety assessment of subterranean parking facilities when confronted with fire incidents.

Lastly, it is important to address certain limitations in the present paper. Specifically, due to computational constraints, a grid sensitivity analysis is not conducted, and the study lacks validation through experimental investigations. Despite these constraints, the study successfully showcases a significant enhancement in the efficiency of the ventilation system. This improvement is reflected in the improved clearance of smoke and enhanced visibility during fire incidents. The accomplishment of the study's primary objective in maintaining a minimum visibility threshold plays a pivotal role in fostering a safer environment for firefighting operations and streamlining evacuation procedures.

Author Contributions: Conceptualization, R.R.; methodology, R.R.; software, R.R.; validation, R.R. and S.A.; formal analysis, R.R. and S.A.; investigation, R.R.; data curation, R.R.; writing—original draft preparation, R.R. and S.A.; writing—review and editing, R.R. and S.A.; visualization, R.R.;

supervision, S.A.; project administration, S.A. All authors have read and agreed to the published version of the manuscript.

Funding: This research received no external funding.

Informed Consent Statement: Not applicable.

Data Availability Statement: No data were collected or utilized in this study. This research is based on a theoretical analysis and does not involve the use of empirical data.

Acknowledgments: We would like to also acknowledge the Sustainable Building Design (SBD) lab at the Faculty of Applied Sciences at the University of Liege and Sapienza University of Rome for the use of workstations during the computation. We would also like to thank Alessandro Corsini, Giovanni Delibra, Nasser Rahif, Farzin Rahif, Amin Khoshkholgh, and Saber Elmi for providing technical materials and assistance. The simulations are performed for a commercial building case study (Hasht Behesht) in Tabriz, Iran.

Conflicts of Interest: The authors declare no conflict of interest. The funders had no role in the design of the study; in the collection, analyses, or interpretation of data; in the writing of the manuscript; or in the decision to publish the results.

Appendix A

This section is allocated to present remaining visibility fields for the base case and proposed fan setups under different fire location scenarios in Figure A1.

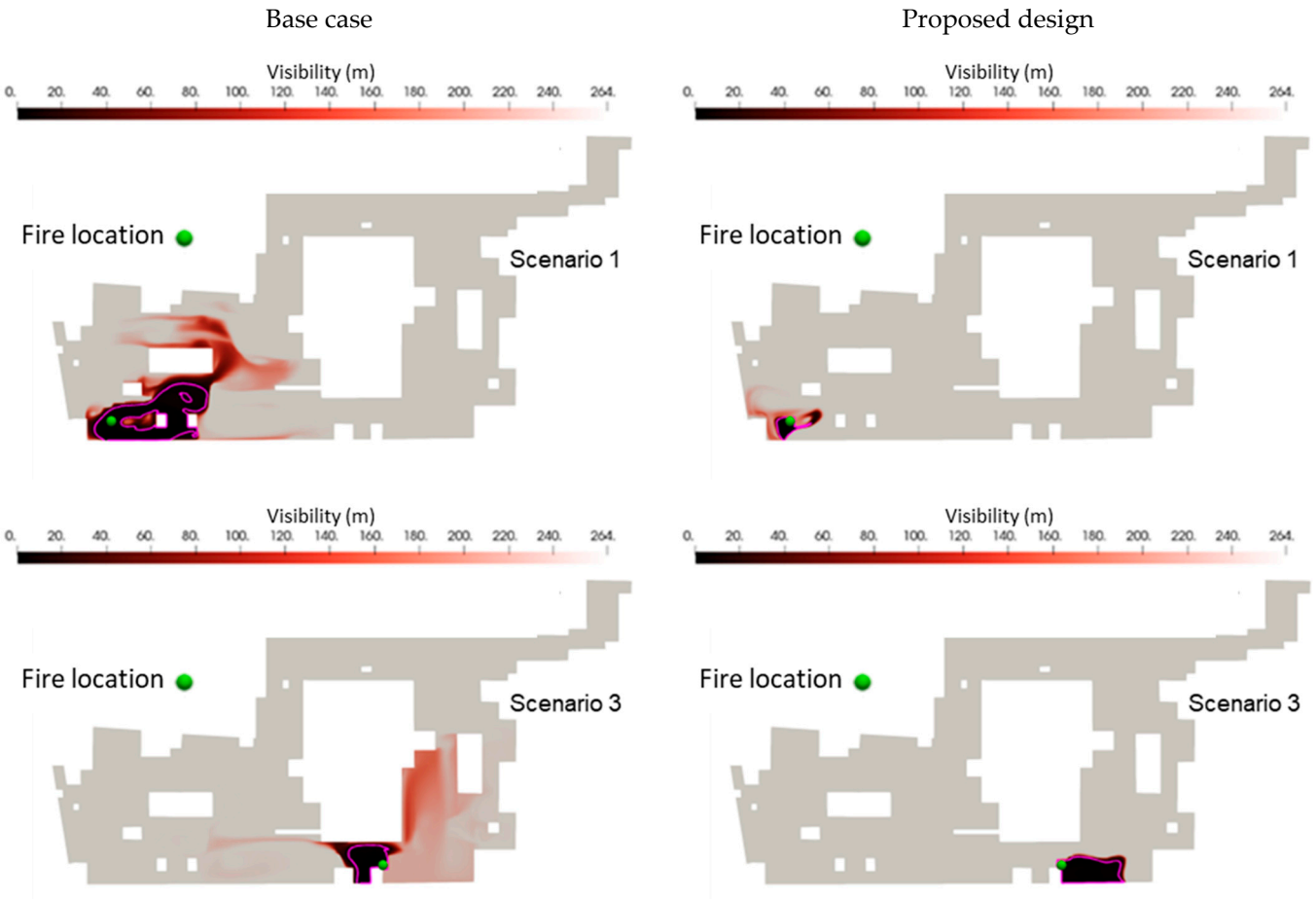

Figure A1. *Cont.*

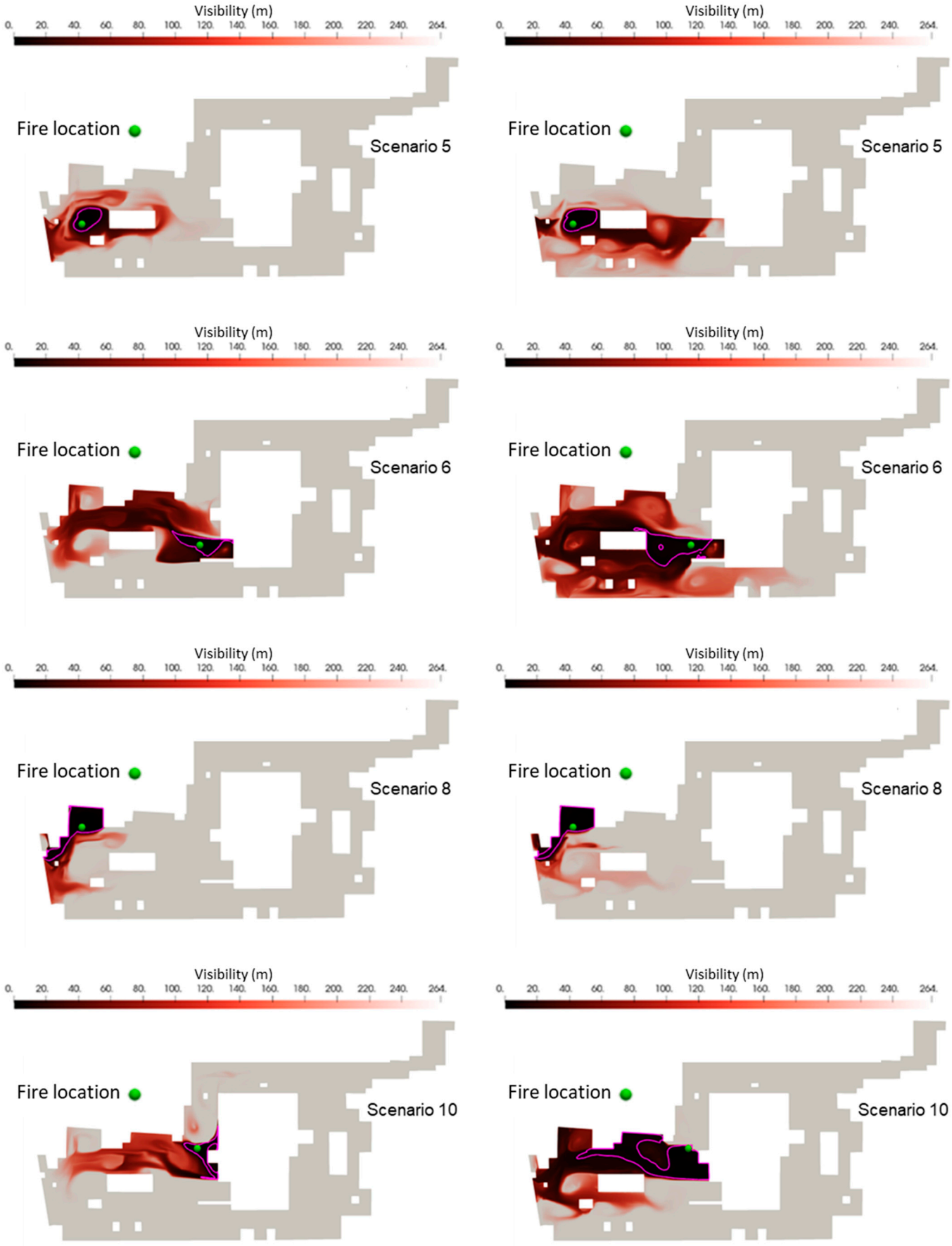

Figure A1. *Cont.*

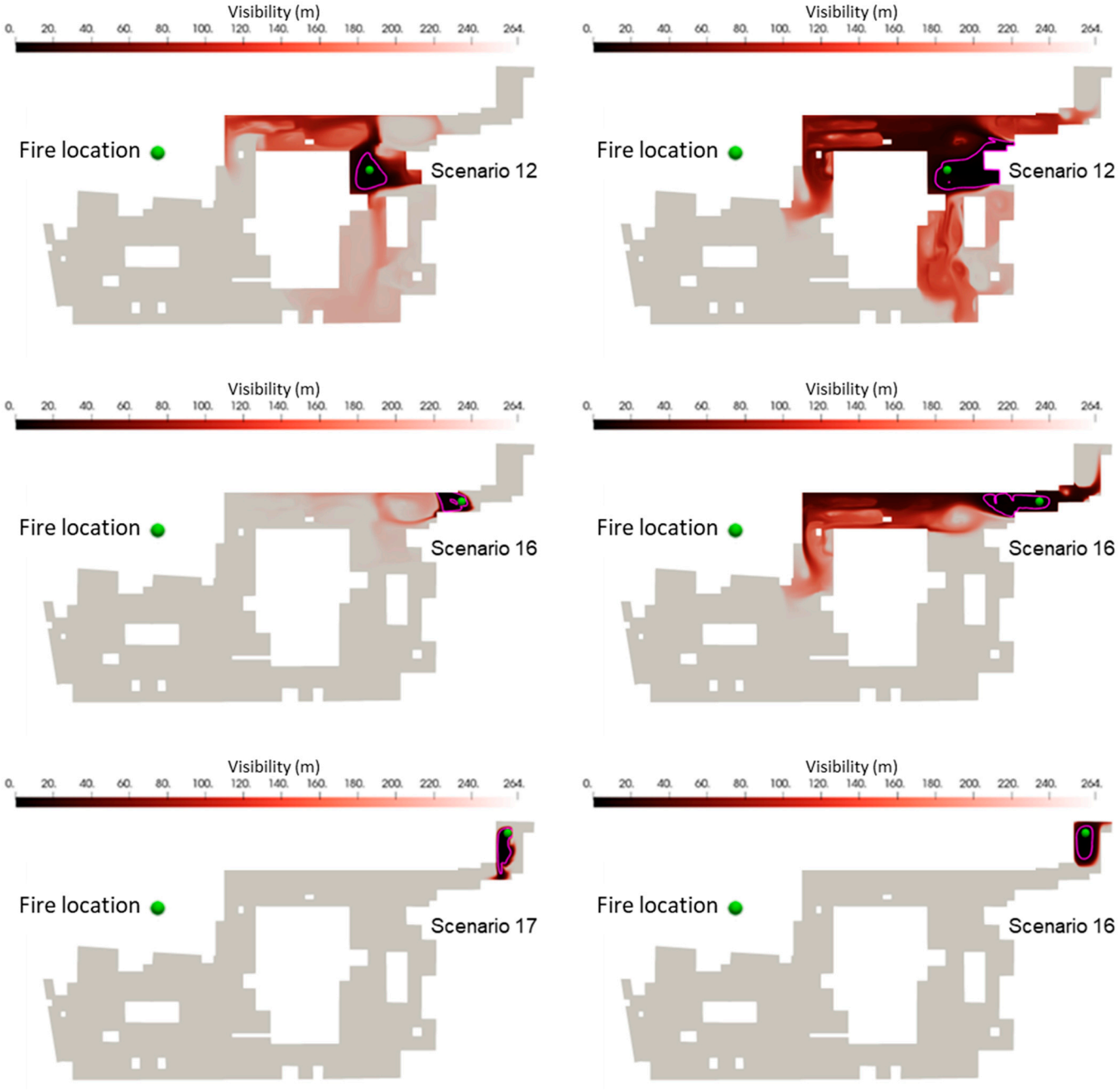

Figure A1. Complementary figures for the visibility distribution for the base case and proposed fan positioning under different fire location scenarios.

References

1. Sulaiman, R.; Din, N.B.C.; Ishak, N.H. Indoor air quality in selected underground car park in malaysia: Studies on ventilation system and the design layout. In Proceedings of the 6th International Conference on Indoor Air Quality, Ventilation and Energy Conservation in Buildings: Sustainable Built Environment, Sendai, Japan, 28–31 October 2007; pp. 28–31.
2. Lu, S.; Wang, Y.H.; Zhang, R.F.; Zhang, H.P. Numerical Study on Impulse Ventilation for Smoke Control in an Underground Car Park. *Procedia Eng.* **2011**, *11*, 369–378. [CrossRef]
3. Viegas, J.C. The use of impulse ventilation to control pollution in underground car parks. *Int. J. Vent.* **2009**, *8*, 57–74. [CrossRef]
4. Kerber, S.; Walton, W.D. *Characterizing Positive Pressure Ventilation using Computational Fluid Dynamics*; US Department of Commerce, National Institute of Standards and Technology: Gaithersburg, MD, USA, 2003.
5. Peeling, J.; Wayman, M.; Mocanu, I.; Nitsche, P.; Rands, J.; Potter, J. Energy Efficient Tunnel Solutions. *Transp. Res. Procedia* **2016**, *14*, 1472–1481. [CrossRef]
6. Demirel, N. Energy-efficient mine ventilation practices. In *Energy Efficiency in the Minerals Industry: Best Practices and Research Directions*; Springer: Berlin/Heidelberg, Germany, 2018; pp. 287–299.

7. Dai, B.; Wang, Q.; Liu, S.; Wang, D.; Yu, L.; Li, X.; Wang, Y. Novel configuration of dual-temperature condensation and dual-temperature evaporation high-temperature heat pump system: Carbon footprint, energy consumption, and financial assessment. *Energy Convers. Manag.* **2023**, *292*, 117360. [CrossRef]
8. Dai, B.; Qi, H.; Liu, S.; Zhong, Z.; Li, H.; Song, M.; Ma, M.; Sun, Z. Environmental and economical analyses of transcritical CO_2 heat pump combined with direct dedicated mechanical subcooling (DMS) for space heating in China. *Energy Convers. Manag.* **2019**, *198*, 111317. [CrossRef]
9. Rahif, R.; Norouziasas, A.; Elnagar, E.; Doutreloup, S.; Pourkiaei, S.M.; Amaripadath, D.; Romain, A.C.; Fettweis, X.; Attia, S. Impact of climate change on nearly zero-energy dwelling in temperate climate: Time-integrated discomfort, HVAC energy performance, and GHG emissions. *Build. Environ.* **2022**, *223*, 109397. [CrossRef]
10. Rahif, R.; Kazemi, M.; Attia, S. Overheating Analysis of Optimized Nearly Zero-Energy Dwelling During Current and Future Heatwaves Coincided with Cooling System Outage. *Energy Build.* **2023**, *287*, 112998. [CrossRef]
11. Norouziasas, A.; Tabadkani, A.; Rahif, R.; Amer, M.; van Dijk, D.; Lamy, H.; Attia, S. Implementation of ISO/DIS 52016-3 for adaptive façades: A case study of an office building. *Build. Environ.* **2023**, *235*, 110195. [CrossRef]
12. Piraei, F.; Matusiak, B.; Verso, V.R.L. Evaluation and Optimization of Daylighting in Heritage Buildings: A Case-Study at High Latitudes. *Buildings* **2022**, *12*, 2045. [CrossRef]
13. Liu, E.; Wang, X.; Zhao, W.; Su, Z.; Chen, Q. Analysis and Research on Pipeline Vibration of a Natural Gas Compressor Station and Vibration Reduction Measures. *Energy Fuels* **2021**, *35*, 479–492. [CrossRef]
14. Chow, W.K. Ventilation design: Use of computational fluid dynamics as a study tool. *Build. Serv. Eng. Res. Technol.* **1995**, *16*, 63–76. [CrossRef]
15. Çakir, M.; Ün, Ç. CFD Analysis of Smoke and Temperature Control System of Car Park Area with Jet Fans. *J. Eng. Res. Rep.* **2020**, *13*, 27–40. [CrossRef]
16. Sittisak, P.; Charinpanitkul, T.; Chalermsinsuwan, B. Enhancement of carbon monoxide removal in an underground car park using ventilation system with single and twin jet fans. *Tunn. Undergr. Space Technol.* **2020**, *97*, 103226. [CrossRef]
17. Sultansu, S.; Ayhan, O. The Cfd Analysis of Ventilation and Smoke Control System with Jet Fan in a Parking Garage. *Int. J. Adv. Eng. Pure Sci.* **2020**, *32*, 89–95. [CrossRef]
18. Nazari, A.; Jafari, M.; Rezaei, N.; Taghizadeh-Hesary, F.; Taghizadeh-Hesary, F. Jet fans in the underground car parking areas and virus transmission. *Phys. Fluids* **2021**, *33*, 013603. [CrossRef] [PubMed]
19. Kmecová, M.; Krajčík, M.; Straková, Z. Designing jet fan ventilation for an underground car park by CFD simulations. *Period. Polytech. Mech. Eng.* **2019**, *63*, 39–43. [CrossRef]
20. Immonen, E. CFD optimization of jet fan ventilation in a car park by fractional factorial designs and response surface methodology. *Build. Simul.* **2016**, *9*, 53–61. [CrossRef]
21. Senveli, A.; Dizman, T.; Celen, A.; Bilge, D.; Dalkiliç, A.S.; Wongwises, S. CFD analysis of smoke and temperature control system of an indoor parking lot with jet fans. *J. Therm. Eng.* **2015**, *1*, 116–130. [CrossRef]
22. Špiljar, Ž.; Drakulić, M.; Schneider, D.R. Analysis of Jet Fan Ventilation System installed in an Underground Car Park with Partition Walls. *J. Sustain. Dev. Energy Water Environ. Syst.* **2018**, *6*, 228–239. [CrossRef]
23. Deckers, X.; Haga, S.; Tilley, N.; Merci, B. Smoke control in case of fire in a large car park: CFD simulations of full-scale configurations. *Fire Saf. J.* **2013**, *57*, 22–34. [CrossRef]
24. UK Government. *Statutory Guidance 'Ventilation: Approved Document F'*; Department for Levelling up, Housing and Communities and Ministry of Housing, Communities & Local Government: London, UK, 2010. Available online: https://www.gov.uk/government/publications/ventilation-approved-document-f (accessed on 6 July 2023).
25. UK Government. *Statutory Guidance 'Fire Safety: Approved Document B'*; Department for Levelling up, Housing and Communities and Ministry of Housing, Communities & Local Government: London, UK, 2010. Available online: https://www.gov.uk/government/publications/fire-safety-approved-document-b (accessed on 6 July 2023).
26. Briggs, W.L.; Henson, V.E.; McCormick, S.F. *A Multigrid Tutorial*; SIAM: Philadelphia, PA, USA, 2000.
27. FlaktWoods. HTJM Aerofoil—Cased Axial Fans HTJM Aerofoil Performance and Electrical Data. 2013. Available online: https://www.flaktgroup.com/en/products/air-movement/fire-safety-fans/ht-axial-fans/ht-jm-aerofoil-axial-flow-fan/ (accessed on 6 July 2023).
28. Fanchi, J.R. (Ed.) Chapter 9—Fluid Flow Equations. In *Shared Earth Modeling*; Butterworth-Heinemann: Woburn, UK, 2002; pp. 150–169. [CrossRef]
29. Rohdin, P.; Moshfegh, B. Numerical modelling of industrial indoor environments: A comparison between different turbulence models and supply systems supported by field measurements. *Build. Environ.* **2011**, *46*, 2365–2374. [CrossRef]
30. Versteeg, H.K.; Malalasekera, W. *An Introduction to Computational Fluid Dynamics: The Finite Volume Method*; Pearson Education: London, UK, 2007.
31. Menter, F.R. Two-equation eddy-viscosity turbulence models for engineering applications. *AIAA J.* **1994**, *32*, 1598–1605. [CrossRef]
32. Heinze, L. *Mathematical Model for Darcy Forchheimer Flow with Applications to Well Performance Analysis*; Texas Tech Univeristy: Lubbock, TX, USA, 2007.
33. Darcy Fochheimer Explanation. 2018. Available online: https://openfoamwiki.net/index.php/DarcyForchheimer (accessed on 24 May 2019).

34. Klote, J.H.; Milke, J.A. *Principles of Smoke Management*; ASHRAE: Peachtree Corners, GA, USA, 2002; Available online: http://fe.hkie.org.hk/FireDigest/Document/Images/20110601103834728/20110601103834728.pdf (accessed on 6 July 2023).
35. Hopkin, C.; Spearpoint, M.; Hopkin, D. A review of design values adopted for heat release rate per unit area. *Fire Technol.* **2019**, *55*, 1599–1618. [CrossRef]
36. *BS 7346-7*; Components for Smoke and Heat Control Systems. Code of Practice on Functional Recommendations and Calculation Methods for Smoke and Heat Control Systems for Covered Car Parks. British Standards Institution: London, UK, 2013.
37. Behrens, T. *OpenFOAM's Basic Solvers for Linear Systems of Equations*; Chalmers, Department of Applied Mechanics: Gothenburg, Sweden, 2009; Volume 18.
38. Darwish, M.; Moukalled, F. *The Finite Volume Method in Computational Fluid Dynamics: An Advanced Introduction with OpenFOAM®and Matlab®*; Springer: Berlin/Heidelberg, Germany, 2016.
39. Patankar, S. *Numerical Heat Transfer and Fluid Flow*; Taylor & Francis: Oxfordshire, UK, 2018.
40. Harlow, F.H.; Welch, J.E. Numerical calculation of time-dependent viscous incompressible flow of fluid with free surface. *Phys. Fluids* **1965**, *8*, 2182–2189. [CrossRef]